

Supplementary Figures

Text S1 to S6

Figures S1 to S6

5 **Text S1.** (a) We have analyzed monthly sea-ice concentration (SIC) data (September to November 2017) from the passive microwave sensors with spatial resolution of 25 km acquired from the National Snow and Ice Data Center (NSIDC) (Data id-G02135, Version 3, <https://nsidc.org/data>). The data were generated using the NASA Team algorithm, which converts satellite derived brightness temperatures to gridded SIC (Cavalieri, D. J., C. L. Parkinson, P. Gloersen, 1997). The sea-ice anomaly for different year was computed relative to the climatology covering the period of 1979-2015. Red rectangle shows the anomalous record lowest sea-ice area and extent observed since three successive years from 2016 to 2018 with the maximum melting occurred in 2017. (b) We analyzed monthly mean sea-ice extent data from NSIDC (Data id-G02135, Version 3) indicating loss of sea-ice that started from September 2016 and continued for the year 2017, 2018 and 2019. (c) We used ocean potential temperature data from global marine Argo atlas (http://www.argo.ucsd.edu/Marine_Atlas.html#) that indicated anomalous upper ocean warming of the Southern Ocean from 2016 to 2018. The potential temperature was spatially averaged over the south of 55°S region encircling the Antarctica. The likelihood for the occurrence of the polynya is quite high with a background of anomalous upper ocean warming and sea-ice loss.

Text S2. In order to analyze the Aqua-MODIS derived net primary production (NPP), we have validated three ocean-color based models such as the vertically generalized production model (VGPM), *Eppley*-VGPM, and carbon-based productivity model (CbPM) for selecting the best model for the study region. We evaluated the performance of these models by comparing with the in-situ NPP estimated using ^{13}C tracer during the Indian scientific expedition to the Southern Ocean in 2009. The locations of in-situ NPP observations during the austral summer (February to April 2009) are presented in figure S2a. The in-situ NPP from 11 observations range from about 85.04 to 923.83 mg C m⁻² day⁻¹. The detail method of ^{13}C measurement was documented in the previous work (Gandhi et al., 2012). The model based NPP values were available in weekly time scale with a spatial resolution of ~4 km (<https://www.science.oregonstate.edu/ocean.productivity>). The pixel values from the models were extracted around each in-situ observation to generate the matchups for the validation strategy, a method adopted by several authors (Babula Jena, 2017; R. Johnson et al., 2013). The comparative statistical analysis suggested that the scatters were much better in the case of *Eppley*-VGPM estimated NPP (Fig. S2c) than those in the case of VGPM (Fig. S2b) and CbPM (Fig. S2d).

30

Text S3. We analysed eddy-resolving model data available from Copernicus Marine Environment Monitoring Service (CMEMS) global analysis and forecast (<http://marine.copernicus.eu/services-portfolio/access-to-products/>, GLOBAL_ANALYSIS_FORECAST_PHY_001_024). The detailed methodology of product generation, and quality control

approaches for this data is given online at <http://cmems-resources.cls.fr/documents/QUID/CMEMS-GLO-QUID-001-024.pdf>. Figure S3 shows depth-latitude cross section of ocean temperature along 4.7°E during (a) September, (b) October, and (c) November 2017.

Text S4. Hydrographic profiles from an Argo float (ID-5904468) located at the edge of the Maud Rise polynya were analyzed for August-December 2017. The Argo data are being generated from the Southern Ocean Carbon and Climate Observations and Modeling (SOCCOM) Project funded by the National Science Foundation, Division of Polar Programs (NSF PLR -1425989), supplemented by NASA, and by the International Argo Program and the NOAA programs. The data are available at <https://www.mbari.org/science/>. Figure S4 provided evidence on the upliftment of thermocline during the formation of polynya.

Text S5. Argo data were utilized to find the linkage between the observed bloom and the ocean pCO₂ condition. The data are available at <https://www.mbari.org/science/>. Low pCO₂ values that reached as low as 372.8 µatm (Figure 4d) corresponding to the bloom occurrence during October-November 2017 (Figure 4a). The pCO₂ values declined during the occurrence of bloom in comparison with the period of no bloom condition in August-September 2017, 2015 and 2016 (Figure 4). The coefficient of correlation (r) between the pCO₂ and chl- a was -0.56 ($p < 0.01$) during August-September 2017 (Figure S4a). The relationship improved ($r = -0.82$, $p < 0.01$) and the spatial pattern closely matched together during the bloom condition in October-November 2017 (Figures S4b and 4a-d). The best relationship observed between the pCO₂ and chl- a when the data was log transformed ($r = -0.94$, $p < 0.01$).

Text S6. Daily sea-ice concentration (SIC) data from the Special Sensor Microwave Imager Sounder (SSMIS) with spatial resolution of 25 km acquired from the National Snow and Ice Data Center (NSIDC) (Data id-G02135, Version 3, <https://nsidc.org/data>). The data were generated using the NASA Team algorithm, which converts satellite derived brightness temperatures to gridded SIC (Cavalieri, D. J., C. L. Parkinson, P. Gloersen, 1997). The accuracy SIC is within 5% of the actual SIC in winter, and within 15% in summer when the melt ponds are present on the sea ice (Fetterer et al., 2016). Several algorithms are available for converting the microwave brightness temperatures of different frequencies to SIC. In higher SIC and thickness (more than 20 cm), the achieved accuracy is found to be better. The detail information about the sensor description, sea-ice processing methods, synoptic coverage, resolution, projection, validation, and the limitations of sea-ice retrieval from passive microwave sensors are given in an earlier article (Fetterer et al., 2016). Figure S6 shows the reappearance of the Weddell Sea and Maud Rise polynya (within the rectangle) from 23 November 2018 to 12 December 2018. The polynya disappeared in 13 December 2018.

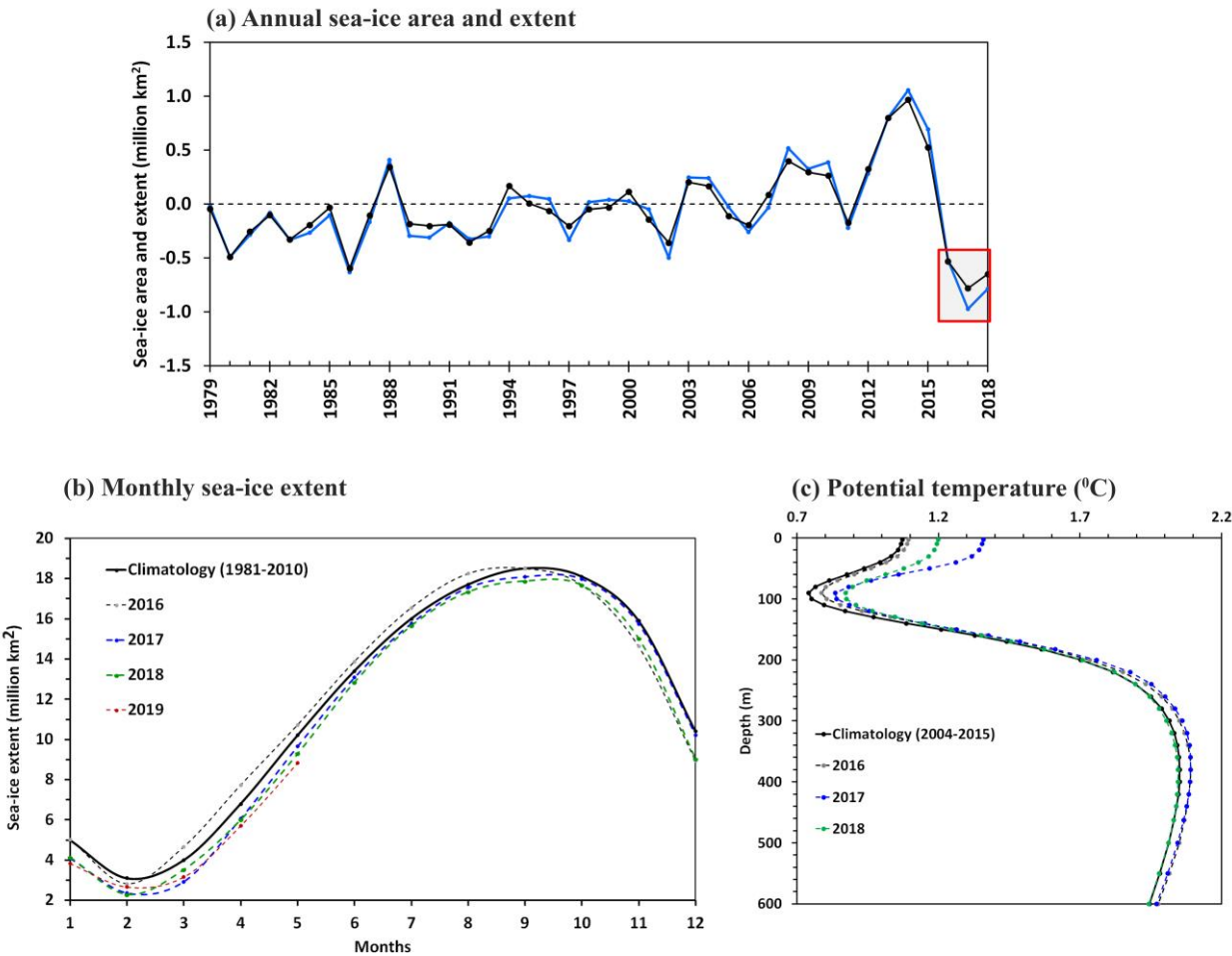


Fig. S1 (a) Inter-annual variability of Antarctic sea-ice area (black) and extent (blue) anomaly relative to the climatology (1979-2015), as analyzed from satellite observations of passive microwave sensors. Red rectangle shows the anomalous record lowest sea-ice area and extent observed since three successive years from 2016 to 2018 with the maximum melting occurred in 2017. (b) Monthly mean sea-ice extent data indicated loss of sea-ice that started from September 2016 and continued for the year 2017, 2018 and 2019. (c) Argo based ocean potential temperature data (2004-2018) indicated anomalous upper ocean warming of the Southern Ocean from 2016 to 2018. The potential temperature was spatially averaged over the south of 55°S region encircling the Antarctica. The likelihood for the occurrence of the polynya is quite high with a background of anomalous upper ocean warming and sea-ice loss.

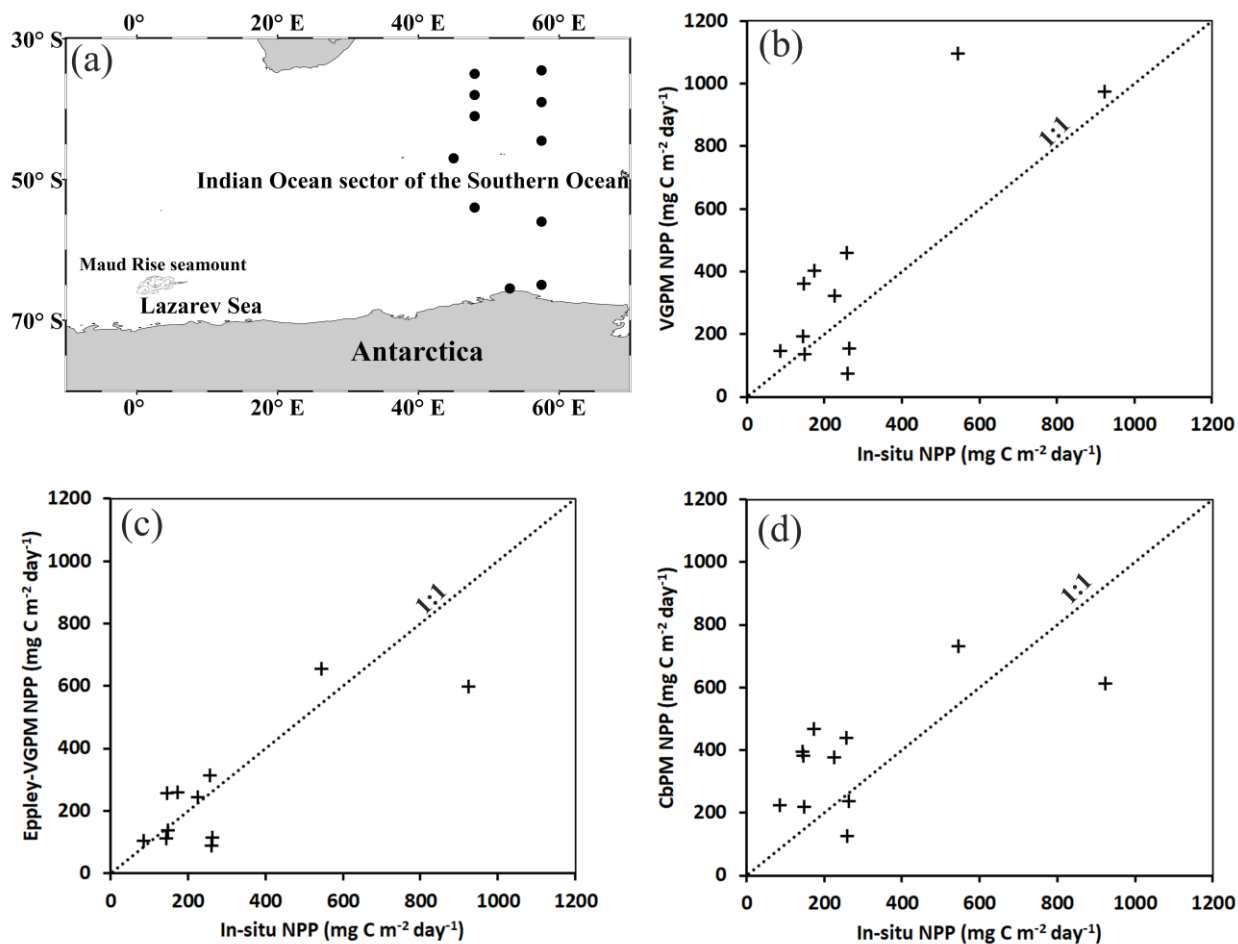
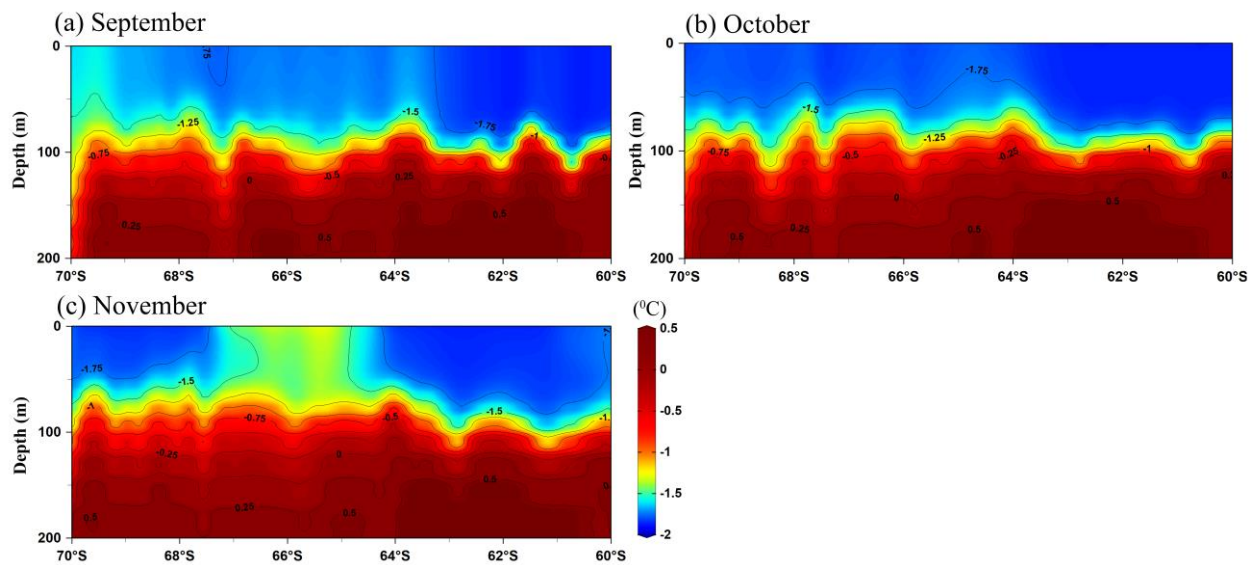


Fig. S2 (a) Filled circles showing the locations of in-situ net primary production (NPP) from ¹³C tracer during the Indian scientific expedition to the Southern Ocean (February to April 2009). Scatter plots between in-situ NPP and (b) VGPM, (c) *Eppeley*-VGPM, (d) CbPM NPP estimations. In-situ measurements had significant positive relationship with the NPP values derived from *Eppeley*-VGPM ($r = 0.82$, $p = 0.001$), VGPM ($r = 0.82$, $p = 0.001$) and CbPM ($r = 0.66$, $p = 0.026$). However, the NPP values from VGPM and CbPM indicating significant overestimations. NPP- net primary production, CbPM- carbon based productivity model, VGPM- vertically generalized production model.



85 **Fig. S3** Depth-Latitude cross section of ocean temperature (along 4.7°E) during (a) September, (b) October, and (c) November 2017, using a high-resolution (1/12°) eddy-resolving model from the Copernicus Marine Environment Monitoring Service (CMEMS).

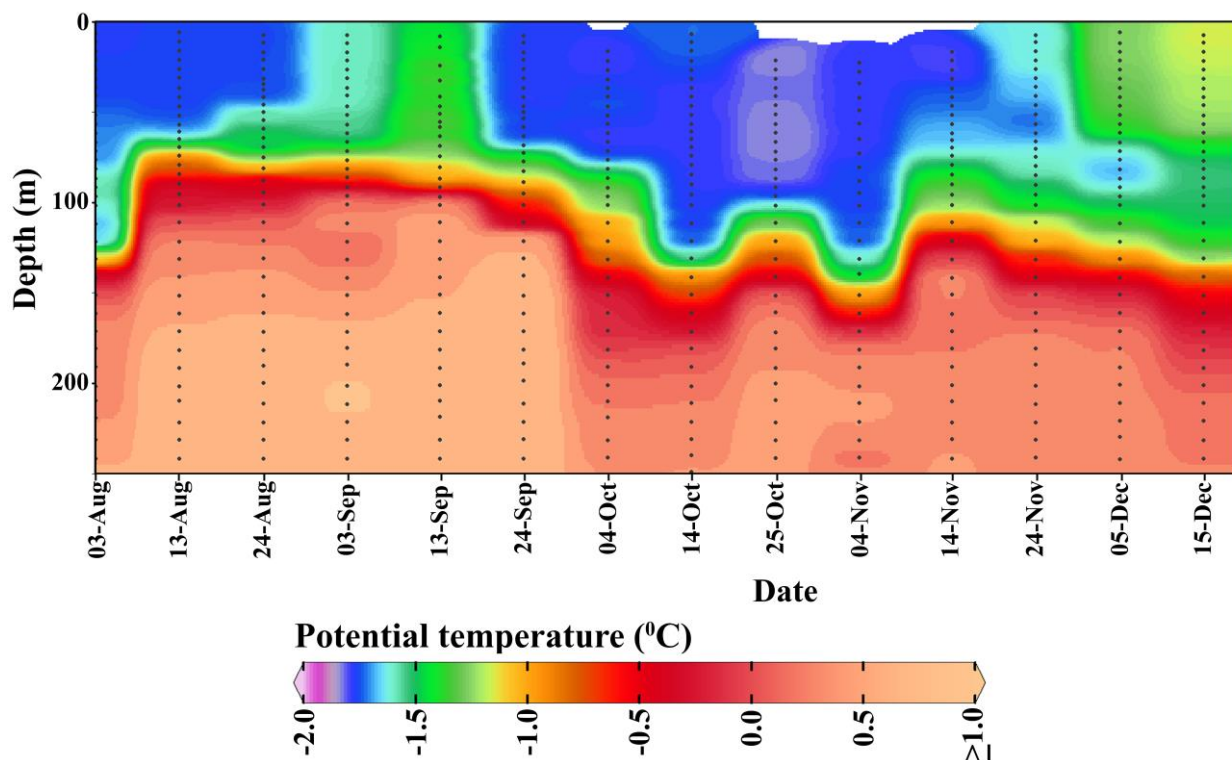


Fig. S4 Profiles from an Argo float (ID-5904468) located at the edge of the Maud Rise polynya during August-December 2017, provided evidence on the upliftment of thermocline.

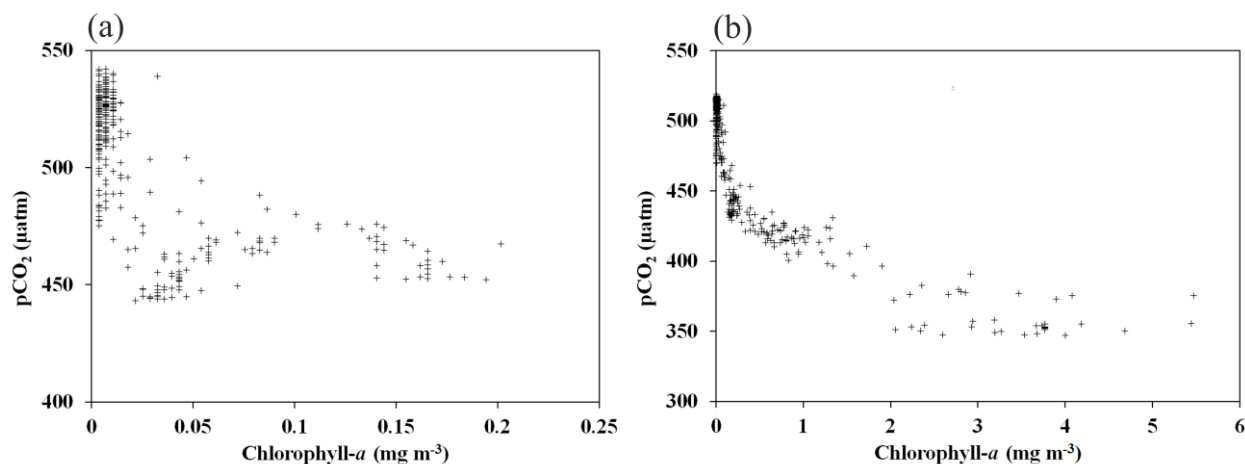


Fig. S5 Argo data were utilized to find the relationship between the chlorophyll-*a* and the oceanic $p\text{CO}_2$ condition. (a) The coefficient of correlation (r) between the $p\text{CO}_2$ and chl-*a* was found to be -0.56 ($p < 0.01$) during August-September 2017.

(b) The relationship improved ($r = -0.82$, $p < 0.01$) during the bloom condition in October-November 2017. The best relationship observed between the $p\text{CO}_2$ and chl- a when the data was log transformed ($r = -0.94$, $p < 0.01$).

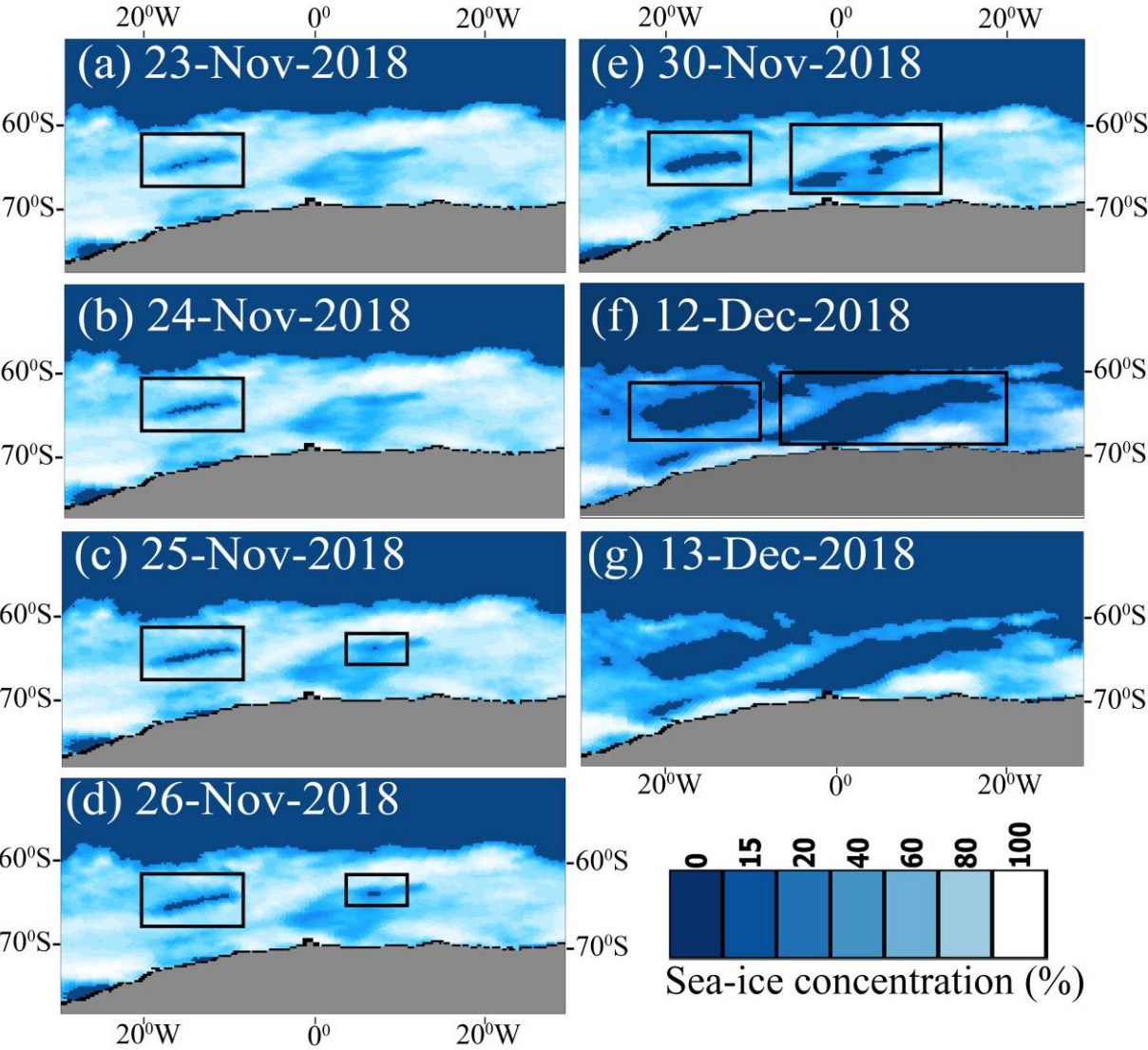


Fig. S6 The Special Sensor Microwave Imager Sounder (SSMIS) shows the reappearance of the Weddell Sea and Maud Rise polynya (within the rectangle) from 23 November 2018 to 12 December 2018. The polynya disappeared in 13 December 2018.